Bundled turbidite deposition in the central Pandora Trough (Gulf of Papua) since Last Glacial Maximum: Linking sediment nature and accumulation to sea level fluctuations at millennial timescale

Stéphan J. Jorry,[1,2] André W. Droxler,[1] Gianni Mallarino,[3] Gerald R. Dickens,[1] Sam J. Bentley,[4] Luc Beaufort,[5] Larry C. Peterson,[6] and Bradley N. Opdyke[7]

Received 28 July 2006; revised 4 June 2007; accepted 17 December 2007; published 29 March 2008.

[1] Since Last Glacial Maximum (23–19 ka), Earth climate warming and deglaciation occurred in two major steps (Bølling-Allerød and Preboreal), interrupted by a short cooling interval referred to as the Younger Dryas (12.5–11.5 ka B.P.). In this study, three cores (MV-33, MV-66, and MD-40) collected in the central part of Pandora Trough (Gulf of Papua) have been analyzed, and they reveal a detailed sedimentary pattern at millennial timescale. Siliciclastic turbidites disappeared during the Bølling-Allerød and Preboreal intervals to systematically reoccur during the Younger Dryas interval. Subsequent to the final disappearance of the siliciclastic turbidites a calciturbidite occurred during meltwater pulse 1B. The Holocene interval was characterized by a lack of siliciclastic turbidites, relatively high carbonate content, and fine bank-derived aragonitic sediment. The observed millennial timescale sedimentary variability can be explained by sea level fluctuations. During the Last Glacial Maximum, siliciclastic turbidites were numerous when the lowstand coastal system was located along the modern shelf edge. Although they did not occur during the intervals of maximum flooding of the shelf (during meltwater pulses 1A and 1B), siliciclastic turbidites reappear briefly during the Younger Dryas, an interval when sea level rise slowed, stopped, or perhaps even fell. The timing of the calciturbidite coincides with the first reflooding of Eastern Fields Reef, an atoll that remained exposed for most of the glacial stages.

Citation: Jorry, S. J., A. W. Droxler, G. Mallarino, G. R. Dickens, S. J. Bentley, L. Beaufort, L. C. Peterson, and B. N. Opdyke (2008), Bundled turbidite deposition in the central Pandora Trough (Gulf of Papua) since Last Glacial Maximum: Linking sediment nature and accumulation to sea level fluctuations at millennial timescale, *J. Geophys. Res.*, *113*, F01S19, doi:10.1029/2006JF000649.

1. Introduction

[2] The Gulf of Papua (GOP) between northeast Australia and south Papua New Guinea (Figure 1) is an outstanding extant example of a tropical mixed siliciclastic/carbonate system [cf., *Mount*, 1984], where large masses of terrigeneous sand and mud discharge into a region of major neritic carbonate production. Unlike mixed systems in the ancient rock record that have received much investigation [e.g., *Budd and Harris*, 1990; *Foreman et al.*, 1991; *Holmes and Christie-Blick*, 1993], only a few late Quaternary analogues have been studied [i.e., *Ferro et al.*, 1999; *Belopolsky and Droxler*, 1999; *Dunbar et al.*, 2000; *Page et al.*, 2003]. The GOP represents an exquisite place to observe, describe, interpret, and ultimately understand the juxtaposition and accumulation of siliciclastic and carbonate sediments within the context of well-established late Quaternary global (eustatic) sea level change [e.g., *Lambeck et al.*, 2002], including major millennial-scale fluctuations in the rate of change [*Weaver et al.*, 2003; *Clark et al.*, 2004].

[3] Sea level and climate clearly influence the nature and timing of sedimentary fill in basins adjacent to continental margins. This is particularly true for turbidites deposited along both siliciclastic [e.g., *Gibbs*, 1981; *Bouma*, 1982; *Mallarino et al.*, 2006] and carbonate [e.g., *Droxler and Schlager*, 1985; *Glaser and Droxler*, 1993; *Schlager et al.*, 1994; *Andresen et al.*, 2003] margins over the last few glacial cycles. The frequency and magnitude of turbidites are generally highest along siliciclastic margins during glacial periods, because the associated lows of sea level expose the shelf, and rivers can transport their sediments

[1]Department of Earth Science, Rice University, Houston, Texas, USA.
[2]Now at Beicip-Franlab Petroleum Consultants, Paris, France.
[3]PanTerra Geoconsultants B.V., Leiderdorp, Netherlands.
[4]Earth Sciences Department, Memorial University of Newfoundland, St. John's, Newfoundland and Labrador, Canada.
[5]Clouds and the Earth's Radiant Energy System, CNRS, Université Aix-Marseille III, Aix-en-Provence, France.
[6]Rosentiel School of Marine and Atmospheric Science, University of Miami, Miami, Florida, USA.
[7]Department of Earth and Marine Sciences, Australian National University, Canberra, Australia.

0148-0227/08/2006JF000649

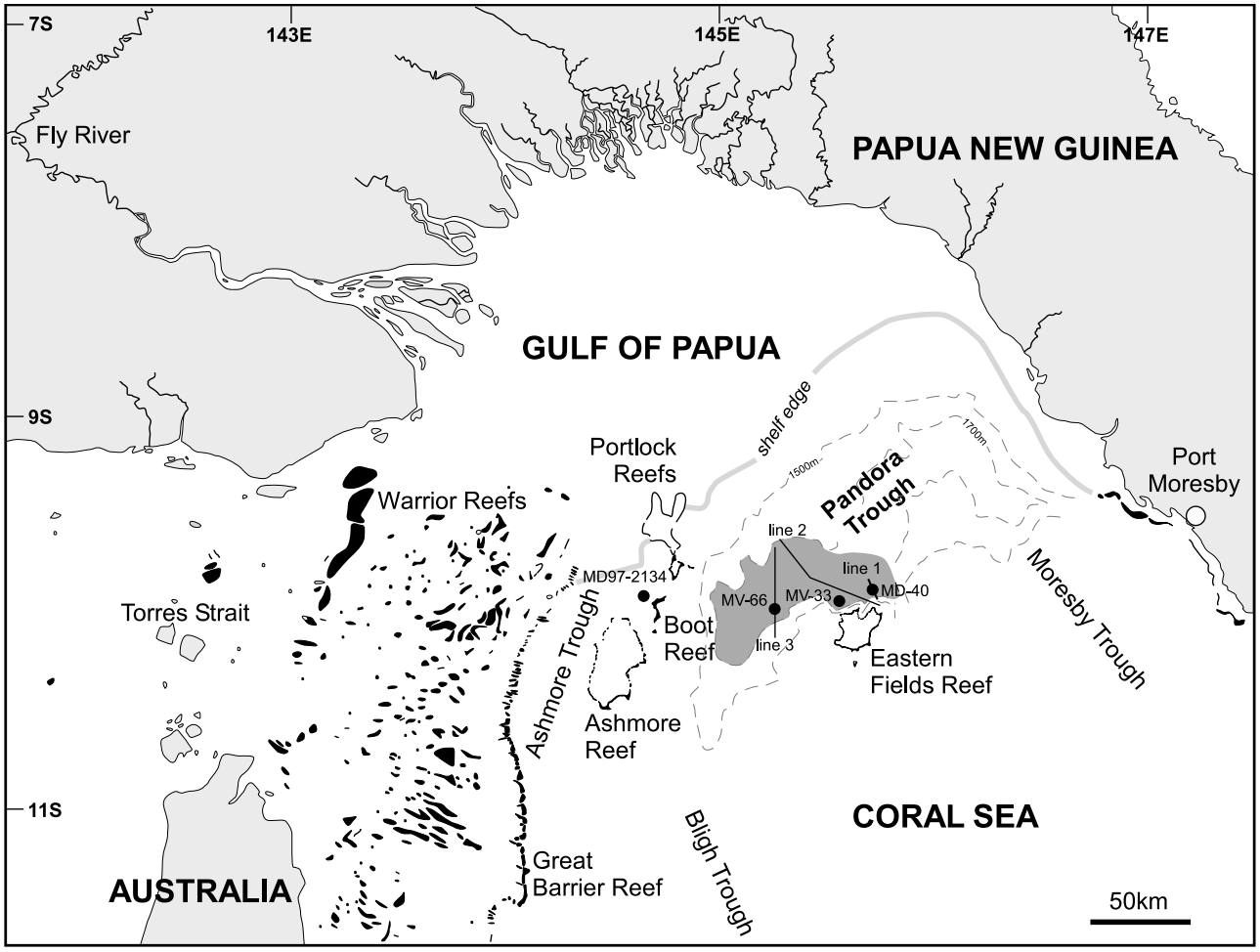

Figure 1. Modern physiography of the Gulf of Papua, and location of the three cores in Pandora Trough (MV-66, MV-33, MD-40) and of core MD97-2134 north of Ashmore Trough. Ashmore and Pandora troughs represent two main oceanic basins directly adjacent to the modern shelf edge. The Pandora Trough is a flat floor basin, mostly enclosed toward the SE (represented by the dark gray area). It is filled with thick siliciclastic sandy/muddy turbidites and slumps alternating with pelagic sediments. The black lines correspond to the location of the 3.5 kHz seismic profiles shown in Figure 2.

directly into the heads of submarine canyons. Conversely, carbonate systems usually show a reversal of this pattern. Calciturbidites preferentially occur during highstands of sea level, when bank tops are flooded and highly productive.

[4] One might expect special sequences of siliciclastic and carbonate turbidites in basins along tropical mixed margins. However, remarkably few studies have examined late Quaternary sediment accumulation in such basins. Most work to date has come from the Belize margin in the Caribbean Sea (B. Carson, personal communication, 2006) and from the Queensland Trough [e.g., *Dunbar et al.*, 2000; *Page et al.*, 2003] adjacent to the Great Barrier Reef (GBR) south of the GOP. These studies have generally selected cores without turbidites and without the age resolution to examine millennial-scale fluctuations during the last glacial cycle. To our knowledge, no study has addressed late Quaternary infill, especially turbidites, along tropical mixed siliciclastic/carbonate margins with millennial timescale resolution.

[5] Pandora Trough parallels the northern shelf edge of the GOP (Figure 1), and receives siliciclastic and carbonate sediment from the adjacent shelf and atolls. The flat floor of central Pandora Trough suggests significant input from sediment gravity flows [*Francis et al.*, 2008]. In this paper, we develop high-resolution stratigraphies for three sediment cores from central Pandora Trough and examine sediment components within the context of late Quaternary sea level change. The cores indicate that Pandora Trough bears the imprint of rapid sea level transgression and regression linked to millennial-scale global warming and cooling since the Last Glacial Maximum (LGM).

2. Background

2.1. Physiography of the Gulf of Papua

[6] The GOP, broadly defined, comprises ~150,000 km^2 of the northern Coral Sea between the southern coast of Papua New Guinea (PNG) and the northeast coast of Australia (Figure 1). The seafloor consists of a half-moon-shaped

continental shelf area of ~40,000 km^2 with a radius of 200 km and a series of slope basins and plateaus covering ~110,000 km^2 [*Francis et al.*, 2008]. Crucial to this paper are the northern and western shelves, isolated carbonate platforms, and Pandora and Ashmore Troughs. A series of large rivers draining PNG annually discharge an enormous load of siliciclastic sediment, perhaps >300 x10^6 metric tones, into the northern GOP [*Pickup and Chewings*, 1983; *Salomons and Eagle*, 1990]. At present, most of this discharge accumulates along the coast, especially the inner shelf [*Harris et al.*, 1993, 1996; *Walsh and Nittrouer*, 2004]. By contrast, the modern middle and outer shelves in the northwest GOP receive little siliciclastic sediment; instead, they are covered by a thin veneer of mostly carbonate sediments with occasional Halimeda bioherms [*Harris et al.*, 1996]. However, numerous channels cut across this portion of the shelf, and many gullies line the upper slope of Pandora Trough [*Harris et al.*, 1993; *Francis et al.*, 2008]. Large masses of siliciclastic sediment almost assuredly crossed the outer central GOP shelf in the recent past.

[7] The northern terminus of the modern GBR occupies the broad western GOP shelf. This complex reef system comprises patch reefs on the inner and middle shelves toward the southern Fly River delta and an almost continuous barrier reef along the shelf/slope break. In both places, reefs have grown to sea level. The GOP also has several large atolls, which include the partially shelf-attached Portlock Reef and Ashmore, Boot, and Eastern Fields reefs. These atolls are typical rimmed reefs, reaching present sea level and enclosing shallow lagoons with water depths of 40–55 m [*Francis et al.*, 2008; J. M. Webster, personal communication, 2006]. Because Holocene lagoonal sediment should have minimal thickness [*MacKinnon and Jones*, 2001; *Gischler*, 2003], the average present lagoon depths most likely approximate the topography of a Pleistocene karstified surface prior to the most recent flooding. These reef systems border Ashmore and Pandora Troughs and supply neritic carbonate sediment to these basins, especially during the Holocene.

[8] Ashmore and Pandora Troughs are adjacent to the shelf. These troughs, in particular the central part of Pandora Trough, are the focus of this study because they represent traps for late Quaternary sediment. The relatively narrow and small Ashmore Trough (Figure 1) lies between the GBR to the west and the atoll chain of Ashmore, Boot, and Portlock reefs to the east. The seafloor of Ashmore Trough dips to the south toward the Bligh Trough and to the east toward Pandora Trough so that it resembles a slope more than a basin per se. Surface sediment is dominated by neritic carbonate shed from surrounding reefs [*Carson et al.*, 2008]. East of Ashmore Trough is the much larger Pandora Trough (Figure 1), a basin bounded by the atoll chain of Ashmore, Boot, and Portlock reefs to the west, the GOP shelf edge to the north, and Eastern Plateau (with the atoll of Eastern Fields) to the south. The eastern end of Pandora Trough is open to Moresby Trough. The central part of Pandora Trough has a very flat seafloor (Figure 2), bathymetry typical for an enclosed basin filled with thick siliciclastic sandy/muddy turbidites and intervening hemipelagic sediments. Northeast of Eastern Fields atoll, Pandora Trough contains drowned parts of a broader Miocene carbonate platform that included Eastern Fields [*Tcherepanov et al.*, 2008]. Features include a series of subparallel ridges hundreds of meters high (interpreted as the unburied and drowned part of the Miocene platform) and several subcircular minibasins about 2 km wide. These are disconnected from the main seafloor of Pandora Trough and partially filled with onlapping sedimentary units, presumably rich in muddy turbidites (Figure 2).

2.2. Late Quaternary Changes in Sea Level and Climate

[9] Over the last 23 ka, Earth systems have experienced two extreme climate end-members and the dramatic transition between them. During the LGM interval ~23–19 ka B.P., sea-surface temperatures dropped by several degrees, even in tropical latitudes [*Thunell et al.*, 1994; *Lea et al.*, 2000; *Guilderson et al.*, 2001; *Visser et al.*, 2003], and eustatic sea level was much lower than at present, probably about −125 m [*Fairbanks*, 1989; *Yokoyama et al.*, 2000; *Weaver et al.*, 2003; *Clark et al.*, 2004; *Bassett et al.*, 2005]. Global climate reached an optimal interglacial regime in the early Holocene ~7–6 ka B.P., when sea level rose to within several m of its present level [*Lambeck and Chappell*, 2001].

[10] The transition from the LGM to the Holocene was not smooth; rather, it involved major changes in rates of warming and sea level rise. The ~12 ka of warming, first initiated at 19 ka B.P. [*Clark et al.*, 2004], was marked by several intervals of stepwise climatic changes, the Bølling-Allerød interval (between 14.5 and 12.5 ka B.P.) and the Preboreal warming at the beginning of the Holocene (11.5 ka B.P.), being the most preeminent of them [*Alley et al.*, 1993]. Two short intervals characterized by more glacial conditions, referred to as the Oldest and Younger Dryas, also occurred ~18–14.7 and ~12.5–11.5 ka B.P., respectively [*Alley et al.*, 1993; *Hughen et al.*, 2000; *Weaver et al.*, 2003]. The temporal and mechanistic links between changes in temperature and sea level during the deglaciation remain controversial [*Kienast et al.*, 2003; *Weaver et al.*, 2003]. Regardless, there were clearly two short intervals of fast sea level change commonly called meltwater pulse 1A (MWP 1A) and meltwater pulse 1B (MWP 1B). During these events, sea level rose by >40 and >11 mm/a (where a is years), respectively [*Weaver et al.*, 2003]. The climate coolings (e.g., Oldest and Younger Dryas) appear coupled to plateaus in the sea level curve [*Hanebuth et al.*, 2000; *Weaver et al.*, 2003]; though not demonstrated or accepted, sea level might have dropped during these intervals [*Liu et al.*, 2004].

3. Materials and Methods

3.1. Core Collection

[11] Three cores from Pandora Trough (Figures 1 and 2, Table 1) were examined in this study. Two jumbo piston cores, MV25-0403-33JPC (MV-33) and MV26-0403-66JPC (MV-66), were collected during the 2004 PANASH cruise aboard R/V *Melville*; one Casq core MD05-2940C^2 (MD-40) was collected during the 2005 PECTEN cruise aboard R/V *Marion Dufresne*. The Casq corer is a 12 m long, 0.25 m width/breadth square section gravity corer, commonly used to obtain sedimentary sequences kept almost intact. Core MV-66 was retrieved from the middle,

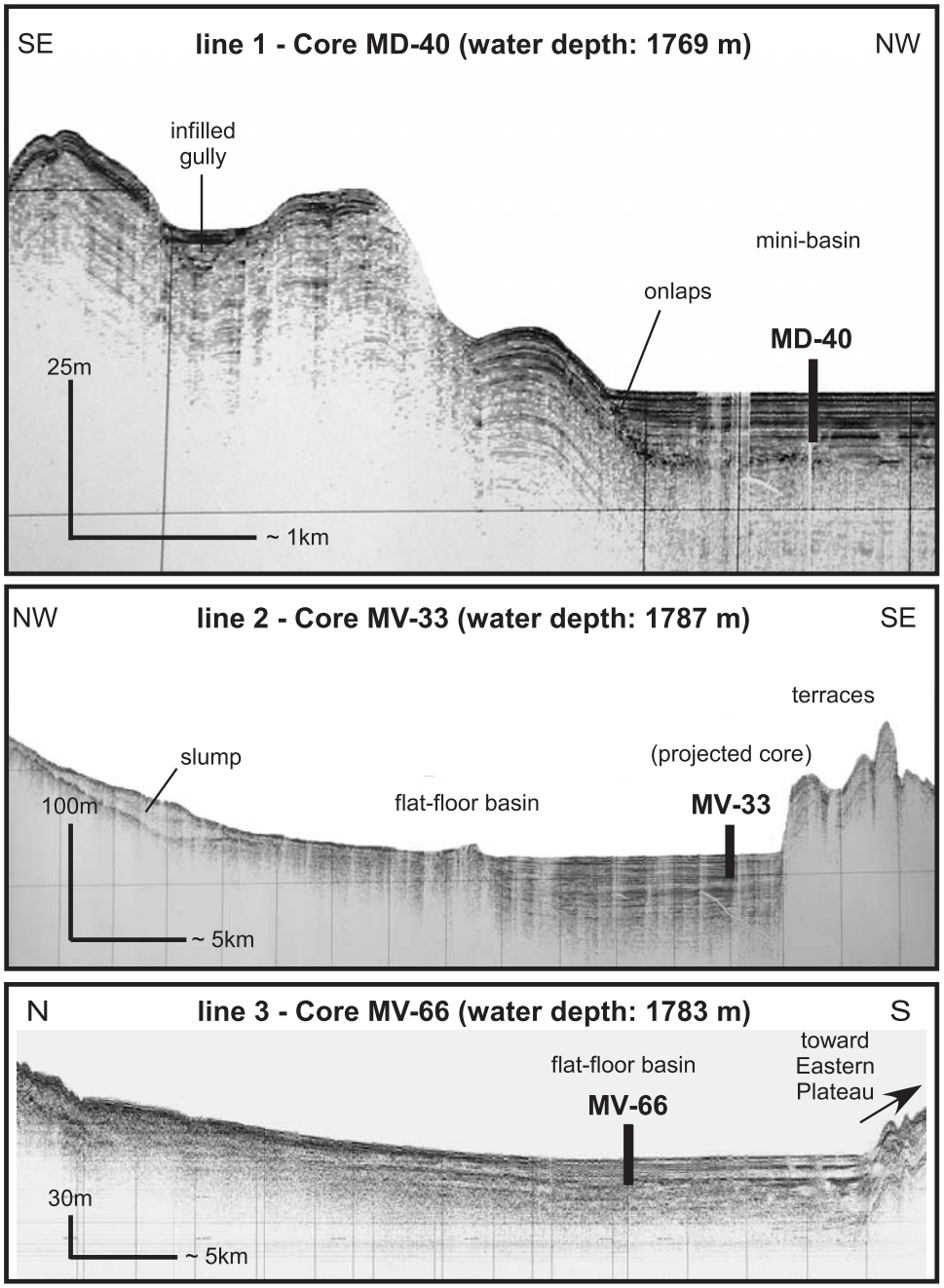

Figure 2. The 3.5 kHz seismic lines crossing the Pandora Trough and location of core MD-40 (flat floor mini basin, north Eastern Fields Atoll) and MV-33 and MV-66 (central Pandora Trough).

flat central portion of Pandora Trough, at mid distance (~75 km) between the atoll chain of Ashmore, Boot, and Portlock to the west and Eastern Fields atoll to the east. Core MV-33 was retrieved in the eastern flat part of central Pandora Trough, 30 km north of Eastern Fields. Core MD-40 is located in one of a series of subcircular, partially isolated minibasins 50 km north of Eastern Fields.

[12] During the 2005 PECTEN cruise, core MD-40 was logged and imaged. Physical and magnetic properties (P wave velocity, gamma density and porosity, magnetic susceptibility) were measured at 2 cm intervals using a Geotek MultiSensor Core Logger. Sediment color was measured at 5 cm steps using a handheld Minolta CM 2002 spectrophotometer. We use lightness (L*), red–green chromaticity (a*) and blue–yellow chromaticity (b*) of the spherical L*a*b* color space. The mean standard deviation for these measurements is 0.06 for L*. The lightness of cores MV-66 and MV-33 was also measured, but at Rosenstiel School of Marine and Atmospheric Science (University of Miami) using a MultiSensor Core Logger.

[13] Preliminary core descriptions were made during both cruises, and detailed descriptions were made during the postcruise sampling. Three main types of sediments were

Table 1. Location, Type, Bathymetry, and Length of the Studied Cores[a]

Core Name	Core Type	Latitude, °S	Longitude, °N	Water Depth, m	Length, m
MV26-0403-66JPC	Jumbo piston core	10.0020	145.1500	1783	11.68
MV25-0403-33JPC	Jumbo piston core	9.8670	145.6000	1787	12.76
MD05-2940C[2]	Casq box core	9.7937	145.7248	1769	8.80

[a]These cores have been retrieved in the turbiditic systems of the Pandora Trough, Gulf of Papua, during a 2004 R/V *Melville* (MV cores) and a 2005 R/V *Marion Dufresne* (MD cores) cruise. MV-66 is located at the middle of the flat floor Pandora Trough, a distal location from Eastern Fields Atoll (75 km). MV-33 has been collected on the flat floor of Pandora Trough, 30 km north of Eastern Fields Atoll. MD-40 has been retrieved in the middle of a flat floor circular minibasin, located 50 km north of Eastern Fields Atoll.

differentiated: siliciclastic sandy and muddy turbidites, calciturbidites, and intervening hemipelagic sediment.

3.2. Size Separations

[14] Each core was sampled at 10 cm intervals, purposely excluding turbidites. Sediment samples were freeze-dried for 48 h to remove pore water. Dried sediments were disaggregated with Calgon solution and sieved with water using a 63 μm mesh. Both fractions were retained and dried again.

[15] The >63-μm fraction was examined under a reflected light microscope to qualitatively assess grain composition. Throughout all three cores, carbonate dissolution is modest and planktic foraminifer tests are abundant in hemipelagic sediment intervals. Specimens are well preserved and show no evidence of mud infilling or diagenetic recrystallization (e.g., secondary carbonate cement). Samples were then dry sieved to retain the >250 μm fraction from which tests of specific planktic foraminifer species were identified and picked for oxygen-isotope analyses (10 tests) and for accelerator mass spectrometer (AMS) ^{14}C dating (500 tests).

3.3. Geochemical Observations

[16] Oxygen-isotope analyses were conducted on small batches of monospecific planktic foraminifera that calcify in the surface mixed layer of the water column: *Globigerinoides ruber* for core MV-66 and *Globigerinoides sacculifer* (without the final sac-like chamber) for core MD-40. On average, 10 specimens were picked from the >250 μm fraction. Specimens were ultrasonically cleaned in distilled water after careful crushing to release potential sediment infilling. Samples were then roasted under vacuum at 375°C for 1/2 h to remove organic contaminants. Using a common 100% phosphoric acid bath at 90°C, 20–50 μg of sample were reacted and analyzed using a GV Instruments Optima isotope ratio mass spectrometer at University of California, Davis. Isotope values are reported in delta notation relative to Vienna Peedee belemnite. Repeated analyses of a marble working standard (calibrated against the international standard NBS-19) indicate an accuracy and precision of 0.05‰ (1σ).

[17] A total of 10 AMS dates were also obtained in cores MV-66, MV-33, and MD-40 (Table 2). For each measurement, about 500 specimens of *G. ruber* and *G. sacculifer* were picked from the >250 μm fraction, washed in an ultrasonic bath with distilled water, and dried. These aliquots were then analyzed at the AMS laboratory at University of California, Irvine. Reported radiocarbon ages were converted to calendar ages using the Radiocarbon Calibration Program [*Fairbanks et al.*, 2005]. A surface ocean reservoir correction of 468 years was used; this is the sum of the global surface water reservoir age correction of 400 years [*Stuiver and Braziunas*, 1993; *Bard et al.*, 1994] and the regional reservoir age correction ΔR of 68 years for Torres Strait [*Reimer and Reimer*, 2001], assuming it to be invariant with time. We also assume that the upper ocean waters (i.e., where *G. ruber* and *G. sacculifer* live) do not vary by >200 years [*Duplessy et al.*, 1991]. All ages are reported in thousands of years before present (ka B.P.), where Present is defined as 1950 AD.

[18] The <63 μm fraction of sediment was used to determine carbonate content and carbonate mineralogy. Carbonate contents were analyzed using a carbonate bomb [*Müller and Gastner*, 1971; *Droxler et al.*, 1988]. About 2 cm of sample were placed into a sealed vessel and reacted with 20% HCl (2.3 mol L^{-1}). The volume of CO_2 released was compared to volumes released by reacting known amounts of 100 percent $CaCO_3$ standard. The precision of the analysis is ~2%.

[19] Carbonate mineralogy was determined on 33 samples by X-ray diffraction (XRD). Samples were ground with an agate mortar and pestle and, depending on the amount, either packed with a spatula into an aluminum sample holder or dispersed in a methanol solution and pipetted onto a glass slide. Analyses were conducted using a Rigaku D/Max Ultima II Powder Diffractometer housed at Rice University. Each sample was scanned twice: at a fast speed of 2°/min from 2 to 100° 2θ for general mineralogy identification and at a low speed of 0.25°/min from 25 to 31° 2θ for optimal resolution of carbonate phases. Differentiation of high magnesium calcite (HMC) and low magnesium calcite (LMC) was based on an established relationship between the d104 lattice spacing shift and mole% $MgCO_3$ [*Goldsmith et al.*, 1961].

[20] Total organic carbon (TOC) content was measured on 88 samples of bulk sediment from core MD-40 using an EC-12 Carbon Determinator manufactured by Leco Corporation. Rock samples were homogenized by grinding and the carbonate carbon was removed by acidification. Residual material was then combusted, and organic-carbon contents were determined from the carbon dioxide produced. Analytical precision depends on sample type and carbon content, but averaged ~0.5% for our samples.

4. Results

[21] Age/Depth models for the three cores have been determined on the basis of at least one of the following glacial/interglacial stratigraphies using down core variations of (1) δ^{18}O in planktic foraminifers *G. sacculifer* or *G. ruber*, (2) carbonate content in the fine fraction (<63μm), and (3) lightness values by digital scans. Moreover, those

Table 2. Radiocarbon Dates From Cores MV-33, MV-66, and MD-40[a]

Core	Depth[b] cmbsf	^{14}C Age (Planktic), years	^{14}C Age (Wood), years	Standard Deviation, years	Corrected ^{14}C Age (Planktic Age Minus 468 Years), years	^{14}C Calendar Age [*Fairbanks et al.*, 2005][c], years
MV-66	62–64	8,390	–	10	7,922	8,722
MV-66	127–129	10,730	–	25	10,262	12,033
MV-66	221–223	13,040	–	80	12,572	14,776
MV-66[d]	837	–	16,450	45	–	19,563
MV-66[d]	955	–	17,100	40	–	20,272
MV-33	154–156	10,625	–	40	10,157	11,837
MV-33	331–333	11,325	–	25	10,857	12,787
MD-40	100–102	10,280	–	20	9,812	11,226
MD-40	180–182	12,280	–	40	11,812	13,724
MD-40	320–322	13,490	–	40	13,022	15,439
MD-40	420–422	15,545	–	45	15,077	18,436
MD-40	700–702	19,190	–	60	18,722	22,349

[a]All dates are based on planktic foraminifer *Globigerinoides ruber* and *Globigerinoides sacculifer* measured at Irvine (University of California, Irvine).
[b]In cmbsf (cm below seafloor).
[c]The ^{14}C ages were converted into calendar ages using the Radiocarbon Calibration Program [*Fairbanks et al.*, 2005].
[d]Two additional (AMS) ^{14}C dates have been obtained from wood fragments at core MV-66 (L. J. Patterson et al., unpublished manuscript, 2008).

stratigraphies are solidly anchored by several ^{14}C AMS dates.

4.1. Primary Core Chronology

[22] As true in many regions [e.g., *Linsley*, 1996; *Dürkoop et al.*, 1997; *Chodankar et al.*, 2005], δ^{18}O records of *G. sacculifer* and *G. ruber* from Coral Sea cores can be correlated to global δ^{18}O records to obtain first-order ages since 100 ka [*Anderson et al.*, 1989; *Dunbar et al.*, 2000; *de Garidel-Thoron et al.*, 2004]. There is, however, an offset between the δ^{18}O of these planktic foraminiferal species, with δ ^{18}O of *G. sacculifer* typically about 0.5 to 0.6‰ heavier than that of *G. ruber* [e.g., *Stott et al.*, 2002]. The δ^{18}O of planktic foraminifera is also associated with changes in local salinity. The modern δ^{18}O salinity relationship in the tropical western Pacific is ~0.2‰ (δ^{18}O) per unit of salinity [*Fairbanks et al.*, 2005], although this relationship varies slightly from region to region and may be lower in the western tropical Pacific, because the summer/winter salinity contrast is low [*Stott et al.*, 2002].

[23] Ages for cores MV-66 and MD-40 were initially determined using down core variations in the δ^{18}O of planktic foraminifers *G. ruber* and *G. sacculifer*, respectively (Figures 3 and 4). The glacial–interglacial transition is clearly identified in both cores. In core MD-40 below 400 cm, the δ^{18}O values of *G. sacculifer* tests range from −0.5 to −1.0‰; the values decrease by −0.4‰ from 400 to 120 cm; above 120 cm, the δ^{18}O values range from −1.4 to −2.3‰. For core MV-66 below 420 cm, the δ^{18}O of *G. ruber* tests range from −1.0 to −1.2‰; they decrease by −0.5‰ from 420 to 130 cm and range from −1.7 to −2.9‰ in the upper 130 cm of the core. The heavy δ^{18}O values in the lower half of each core clearly correspond to the LGM (>23 ka B.P.), the light δ^{18}O values in the upper 30 cm correspond to Holocene (<11 ka B.P.), and the intermediate δ^{18}O values characterize the deglacial transition. In both records, the δ^{18}O amplitude from the LGM to Holocene is the same 1.8‰ for MD 40 and 1.9‰ for MV-66, though the δ^{18}O values in core MV-66 are systematically 0.6‰ lighter than in core MD-40.

[24] The oxygen isotope stratigraphies for cores MD-40 and MV-66 nicely correlate with the high-resolution δ^{18}O record from core MD97-2134 (Figure 3). Core MD97-2134 was retrieved at 760 m water depth in northern Ashmore Trough (latitude: 9°54′S, longitude: 144°39′E, Figure 1). Well anchored time wise on 13 AMS dates, *de Garidel-Thoron et al.* [2004] have constructed a high-resolution oxygen-isotope stratigraphy on the basis of *G. ruber* planktic foraminifer shells. By comparison with the MD97-2134 δ^{18}O LGM–Holocene transition which display an amplitude of about 2‰, LGM is clearly identified in core MD-40 at ~650–700 cmbsf (cm below seafloor), which depth corresponds to the heaviest δ^{18}O values, i.e., −0.45 per mil Peedee belemnite (Figure 3).

[25] The glacial_interglacial transitions in cores MD-40 and MV-66, solidly anchored by 8 ^{14}C AMS dates of mixed *G. ruber* and *G. sacculifer* planktic foraminifers (Table 2, Figure 4), confirmed that these cores span from LGM to late Holocene and are recording the last glacial-to-interglacial

Figure 3. Millennial timescale sedimentary variability observed during the last deglaciation in central Pandora Trough. (a) Oxygen isotope curve of the last deglaciation for core MD97-2134, north Ashmore Trough (after *de Garidel-Thoron et al.* [2004], copyright 2004 National Academy of Sciences, U.S.A.). (b) Planktic oxygen isotopes and timing of gravity-flow deposits at core MD-40 since LGM in Pandora Trough. (c) Oxygen isotope record from the Greenland Ice Sheet Project 2 (GISP2) [*Grootes et al.*, 1993; *Stuivert and Grootes*, 2000]. LGM is the Last Glacial Maximum, OD is the Oldest Dryas, B-A is the Bølling-Allerød warming, and YD is the Younger Dryas cold period. (d) Relative sea level (RSL) records from far field sites (*Weaver et al.* [2003], reprinted with permission from AAAS). Data are from Bonaparte Gulf (open circles with lines) [*Yokohama et al.*, 2000], Barbados U/Th-dated corals (open squares) [*Bard et al.*, 1990], Sunda Shelf (open circles with pluses) [*Hanebuth et al.*, 2000], Tahiti (solid triangles) [*Bard et al.*, 1990], and New Guinea (solid squares) [*Edwards et al.*, 1993].

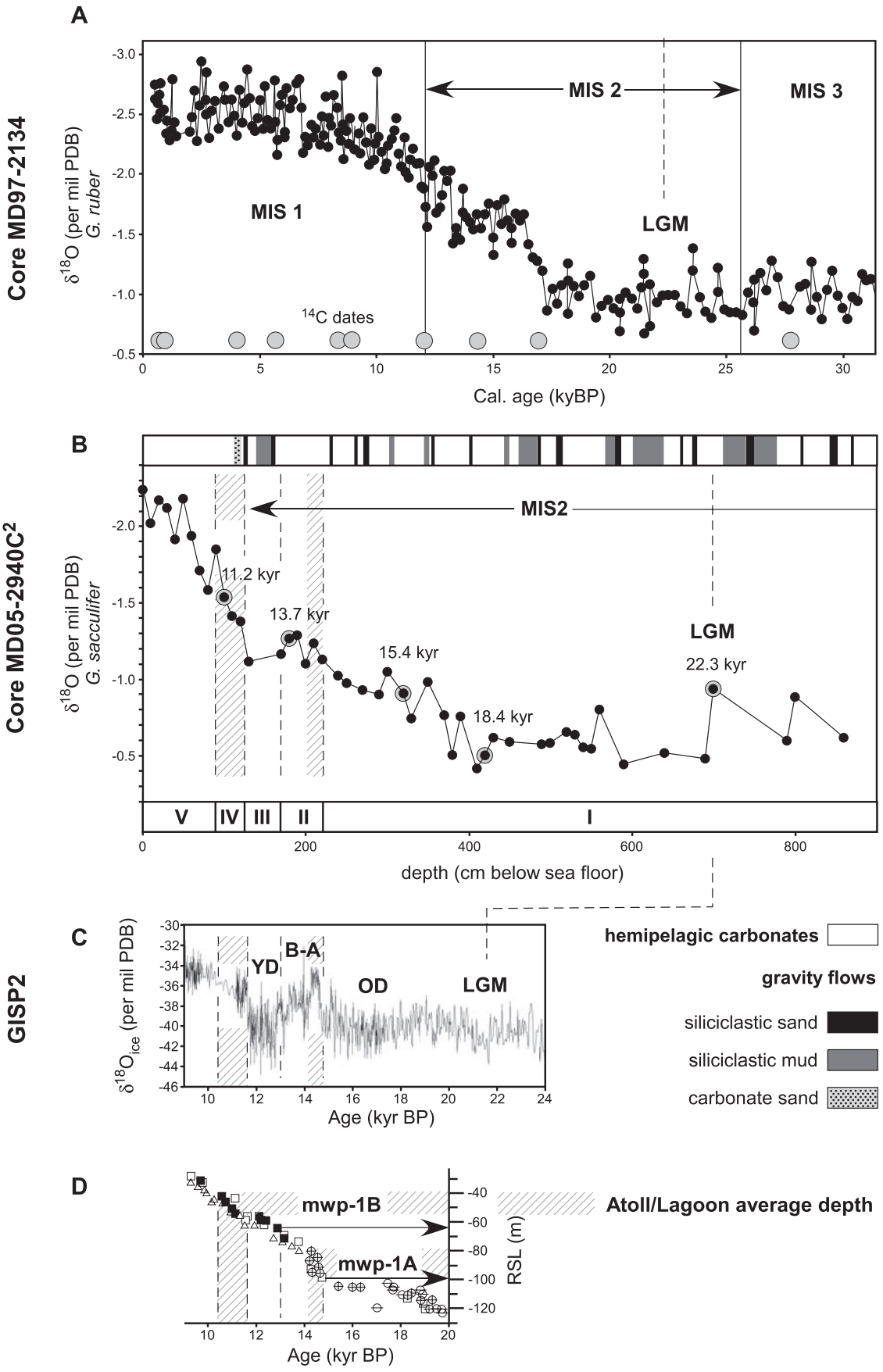
A
Core MD97-2134
δ18O (per mil PDB) G. ruber
MIS 1
MIS 2
MIS 3
LGM
14C dates
Cal. age (kyBP)
B
Core MD05-2940C2
δ18O (per mil PDB) G. sacculifer
MIS2
11.2 kyr
13.7 kyr
15.4 kyr
18.4 kyr
LGM
22.3 kyr
V
IV
III
II
I
depth (cm below sea floor)
C
GISP2
δ18Oice (per mil PDB)
YD
B-A
OD
LGM
Age (kyr BP)
hemipelagic carbonates
gravity flows
siliciclastic sand
siliciclastic mud
carbonate sand
D
mwp-1B
mwp-1A
RSL (m)
Atoll/Lagoon average depth
Age (kyr BP)

Figure 3

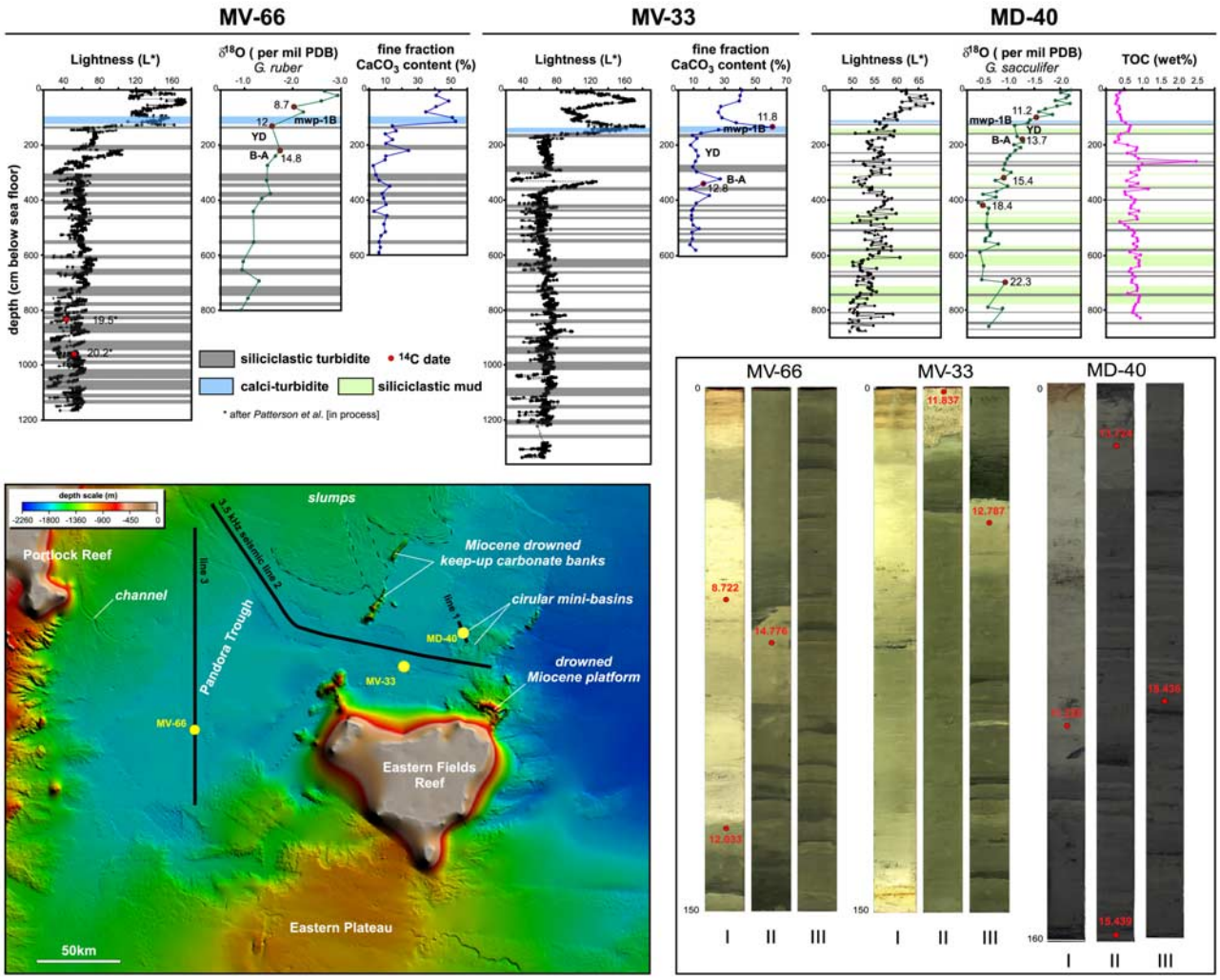

Figure 4. Correlation between cores MV-33, MV-66, and MD-40 based on sedimentological description and measurements of lightness, carbonate content, and oxygen isotopes, anchored by AMS ^{14}C dates. This correlation demonstrates that the last glacial-interglacial transition was a two-steps change from LGM to the Holocene. The first warming/deglacial step corresponds to the Bølling-Allerød/MWP 1A interval. The second step, clearly identified on the three cores by an abrupt decrease of the δ^{18}O, peaks of lightness and carbonate content, and deposition of a calciturbidite, corresponds to the beginning of the Holocene or MWP 1B (Pleistocene/Holocene transition). The location map of these cores results from the integration of multibeam and 3.5 kHz seismic surveys [*Francis et al.*, 2008].

transition or deglaciation. Two additional AMS dates of organic particles from two LGM and late Glacial (late LGM) siliciclastic turbidites in core MV-66 (L. J. Patterson et al., Petrological and geochemical investigations of deep sea turbidite sands in the Pandora and Moresby Troughs: Source to Sink Papua New Guinea focus area, unpublished manuscript, 2008; see also Table 2) confirm a high sediment accumulation rate during the LGM and until the first clear initiation of the last deglaciation (Figure 4).

4.2. Detailed Lithochronology

[26] Although they are separated by distances of tens of km, cores MV-33, MV-66 and MD-40 exhibit a common sediment pattern; siliciclastic sandy turbidites and muddy turbidites are numerous in the lower parts of the cores corresponding to LGM. The turbidites are separated by intervening intervals rich in pelagic carbonates, which become more frequent up the core. The siliciclastic turbidites disappear up the cores and are not recognized in the Holocene, which consists only of pelagic carbonate-rich sediment. Once the siliciclastic sandy turbidite layers disappear in the core, 1 dm thick calciturbidite is observed on the upper part of the three cores (Figure 4).

[27] Siliciclastic turbidites, with dark sand-dominated layers (1–10 cm thick) and well-preserved wood and plant fragments (Figure 5a) and characterized by erosional bases were studied in details in core MD-40. The coarse fraction of these siliciclastic turbidites (from 63 to 125 μm) is dominated by silica and some volcanic-rock-related minerals (i.e., amphibole, pyroxene, zircon, apatite) (Figure 5b). Additional information on the sandy turbidite layers in core MV-66 was found by L. J. Patterson et al. (unpublished manuscript, 2008). The sands at the bases of the turbidite layers are predominantly quartzofeldspathic with a signifi-

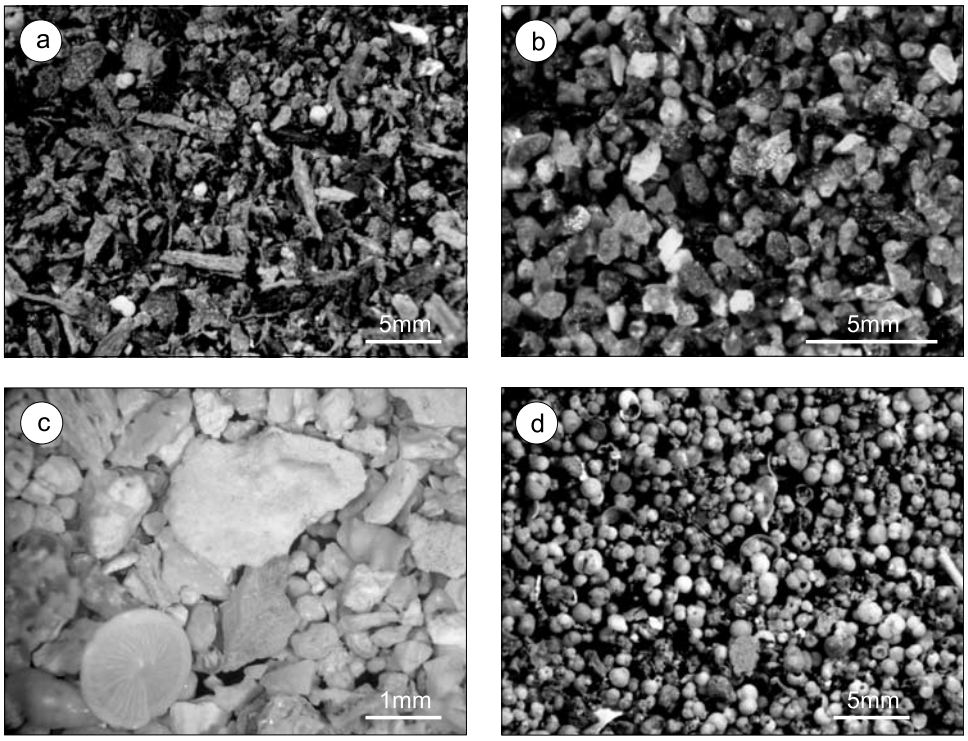

Figure 5. Photomicrographs of sediment accumulated in Pandora Trough. (a) Coarse fraction (>200 and <300 μm) of a siliciclastic turbidite showing an important concentration of wood debris (core MD-40); (b) coarse fraction (>63 and <125 μm) of a siliciclastic turbidite composed of silica and some volcanic-rock-related minerals (core MD-40). (c) Coarse fraction (>300 μm) composed of neritic carbonate fragments and large benthic foraminifers taken at the base of a calciturbidite (core MV-33); d: coarse fraction (>200 and <300 μm) of a pelagic carbonate sediment dominated by planktic foraminifers (core MD-40).

cant amount of heavy minerals (zircon, amphibole, and oxide minerals). Planktic foraminifers are uncommon and are mainly represented by sparse *Orbulina universa*. Benthic foraminifers (*Cibbicides*, *Uvigerina*, *Quinqueloculina*, *Bolivina, Bulimina, Textularia*), gastropods, scaphopods, and diverse bioclastic carbonate fragments are also present in the coarse fraction (>350 μm).

[28] Calciturbidites occur at 130, 160, and 110 cmbsf, in cores MV-66, MV-33, and MD-40, respectively. This calciturbidite is particularly developed in core MV-33, where it displays a well-individualized fining-upward carbonate 20 cm thick layer. The lower part of the calciturbidite consists of heterogeneous skeletal fragments, centimeter to many centimeters in size. Those neritic grains (mostly large benthic foraminifers, gastropods, large bivalve, and echinoid fragments) demonstrate that they had to be produced in shallow water environments of an adjacent carbonate platform, most likely Eastern Fields atoll (Figure 5c). The upper part of the calciturbidite layer in MV-33 consists of mostly planktic foraminifers. In core MV-66, retrieved from a more distal location relative to Eastern Fields, the calciturbidite is thinner and the calcareous particles consist almost exclusively of planktic foraminifers as in the upper part of the calciturbidite in core MV-33. The occurrence of much aragonite and magnesium calcite in the fine fraction of the calciturbidite in both cores MV-33 and MV-66 points to a neritic source for the turbidite material, Eastern Fields Reef being the most likely candidate.

[29] Occurrences of muddy terrigeneous intervals were distinguished in core MD-40 from pelagic intervals mostly by the lack of foraminifers. The deposition of these layers, devoid of foraminifers and other biogenic particles, is interpreted to represent low-density gravity flows [*Mallarino et al.*, 2006] and/or distal or lateral turbidite-mud deposition in Pandora Trough.

[30] Pelagic carbonate-rich intervals contain higher numbers of planktic foraminifers (Figure 5d). Several species and genera have been recognized: *Globigerinoides ruber*, *Globigerinoides sacculifer*, *Globigerina bulloides*, *Orbulina universa*, *Globorotalia menardii*, *Pulleniatina*, *Neogloboquadrina*, *Hantkenina*. These intervals are intercalated with siliciclastic sandy/muddy turbidites through LGM and become the majority of the sediment in the Holocene.

[31] Once primary stratigraphies were established in cores MV-66, MV-33, and MD-40 on the basis of planktic $\delta^{18}O$ down core records anchored on 10 ^{14}C AMS radiocarbon dates (see first paragraph in Results), it became obvious that input of siliciclastic sandy and muddy intervals were dominant during LGM. Frequency and thickness of siliciclastic turbidites progressively decrease up the cores and completely disappear in the Holocene. Between 14.5 and

12.5 ka B.P., the siliciclastic turbidites dramatically turned into an interval that is strictly dominated by the deposition pelagic carbonate_rich sediments. An interval between 12.5 and 11.5 ka B.P. is dominated by the deposition of siliciclastic mud. The base and top of this interval are defined by siliciclastic turbidites observed in all three cores studied in Pandora Trough. Siliciclastic turbidites disappear in the central part of Pandora Trough at the beginning of the Holocene. This interval is marked by the occurrence of a calciturbidite. This calciturbidite most likely represents the initiation of neritic carbonate production. The Holocene is strictly dominated by the deposition of pelagic carbonates enriched by bank-derived fine aragonite.

[32] TOC content varies between 0.25% and 2.49% in core MD-40 (Figure 4). The highest TOC values (2.49 wt%) coincide with siliciclastic turbidites, whereas low values generally characterize pelagic carbonate-richer intervals. TOC values range are 0.5–1.0% during LGM and late Glacial, and <0.5% during the Holocene. In this study, the most plausible explanation for TOC-rich intervals is increased supply of terrigeneous organic matter, especially because most of these intervals in core MD-40 contain many wood and plant fragments (Figure 5a). These fragments are preferentially accumulated during LGM and late Glacial, intervals coinciding with a reduced continental shelf area and, therefore, with a relative proximity of the coastlines.

4.3. Two-Step LGM-Holocene Transition

[33] Although the glacial-interglacial transition in Pandora Trough is clearly recorded by the planktic $\delta^{18}O$ variations, other parameters such as carbonate content and L* (Lightness) variations also illustrated the last glacial-interglacial transition. Carbonate content in cores MV-33 and MV-66 ranges between 3% during LGM and 40–50% in the late Holocene (Figure 4). It is not a surprise that the variations of L* values, directly linked to the carbonate content, also demonstrate the last glacial_interglacial transition; the lowest L* values occur during the LGM and high values during the late Holocene (Figure 4). The good agreement between variations of planktic oxygen-isotope values, lightness, and carbonate concentration, therefore, provide a record of the last deglaciation.

[34] L* of the sediments was measured along the cores at a high sample resolution (every 5 cm or less), and the curves demonstrate that the last glacial-interglacial transition was not smooth but rather was a two-step change from LGM to the Holocene. Pelagic sediment (high L* values at 225 cm in core MV-66, at 338 cm in core MV-33, and at 200 cm in core MD-40), devoid of sandy and muddy turbidites and enriched in foraminifer concentration, marks a first step in each core at the beginning of the deglaciation. This lighter interval, corresponding to higher carbonate content (24% and 27% in cores MV-66 and MV-33, respectively) and lighter $\delta^{18}O$ values, is even more conspicuous because it is abruptly overlain by a core interval characterized by low L* and carbonate values ($CaCO_3$ content drops to 8%), and relatively higher $\delta^{18}O$ values (Figure 4). The beginning and end of this darker interval is framed by the occurrence of two siliciclastic sandy turbidites separated by an unusually muddy interval almost completely devoid of foraminifers. This darker interval is then, followed by a second step with increased L* and carbonate and lighter $\delta^{18}O$ values. This second step is emphasized by some of the highest L* and carbonate values observed in each core, in particular at 116 and 134 cmbsf in cores MV-66 and MV-33, respectively (Figure 4). These highest L* values and $CaCO_3$ peaks correspond to the occurrence of a calciturbidite.

[35] This two-step deglaciation is relatively well anchored in time by radiocarbon dates (Figure 4). The overall deglacial trend, expressed by a relatively gradual decrease of $\delta^{18}O$ values, is interrupted by a significant cold reversal (beginning abruptly at ~12.5 ka B.P. and ending at ~11.5 ka B.P., interval III in Figure 3), underlain and overlain by two stepwise warming periods occurring at ~14.5 and ~11.5 ka B.P. The timing of this cold reversal, as indicated by a significant increase of $\delta^{18}O$ values, low lightness and carbonate content, corresponds relatively well to the timing of the Younger Dryas.

[36] The first warming/deglacial step (interval II in Figure 3), evidenced by low $\delta^{18}O$ values, high $CaCO_3$ content and high L* values, corresponds most likely to the Bølling-Allerød interval during which the MWP 1A occurred (Figures 3 and 4). In core MD-40, a ^{14}C age of 13.7 ka B.P. precisely indicates this warming event. In core MV-33, a ^{14}C age of ~13 ka B.P. supports this pelagic interval as the same warming event. In core MV-66, this event is dated at 14.8 ka B.P., which is older than the two other cores. This older radiocarbon age could be explained by significant erosion of the upper part of the Bølling-Allerød interval during the emplacement of an overlying turbidite layer.

[37] The second warming/deglacial step, identified in the three cores by an abrupt decrease of the $\delta^{18}O$ and peaks of lightness and carbonate content (interval IV in Figures 3 and 4), corresponds to the beginning of the Holocene or MWP 1B. In the three cores, this Pleistocene/Holocene transition is marked by the deposition of a calciturbidite and the accumulation of bank-derived aragonite in the fine carbonate fraction. On the basis of ^{14}C ages obtained in cores MV-66 and MD-40, the timing of the calciturbidite deposition appears synchronous at the scale of the Pandora Trough and to have occurred between 11.5 to 11.0 ka B.P.. The ^{14}C age of 11.8 ka B.P. in core MV-33, obtained from the upper part of the carbonate gravity flow, suggests a possible reworking of older biogenic carbonate particles.

5. Discussion

[38] In the three cores MV-33, MV-66, and MD-40, a series of five distinct intervals at millennial timescale are observed during the last deglaciation (Figure 3). Using the oxygen-isotope curve established on core MD-40, these five intervals, labeled up the core from I to V, can be correlated with the GISP2 oxygen-isotope curve and in respect to the sea level curve of *Weaver et al.* [2003]: (1) Interval I, LGM and late Glacial (including the Oldest Dryas): sandy and muddy intervals with siliciclastic turbidites; (2) interval II, Bølling-Allerød/MWP 1A (~15.0 or 14.5–12.5 ka B.P.): pelagic interval devoid of sandy and muddy siliciclastic turbidites with relatively high carbonate content (foraminifers and coccoliths); (3) interval III, Younger Dryas (between 12.5 and 11.5 ka B.P.): terrigeneous mud-rich interval with a few thin sandy siliciclastic turbidites; (4) interval IV, MWP 1B (11.5–10.5 ka B.P.): return

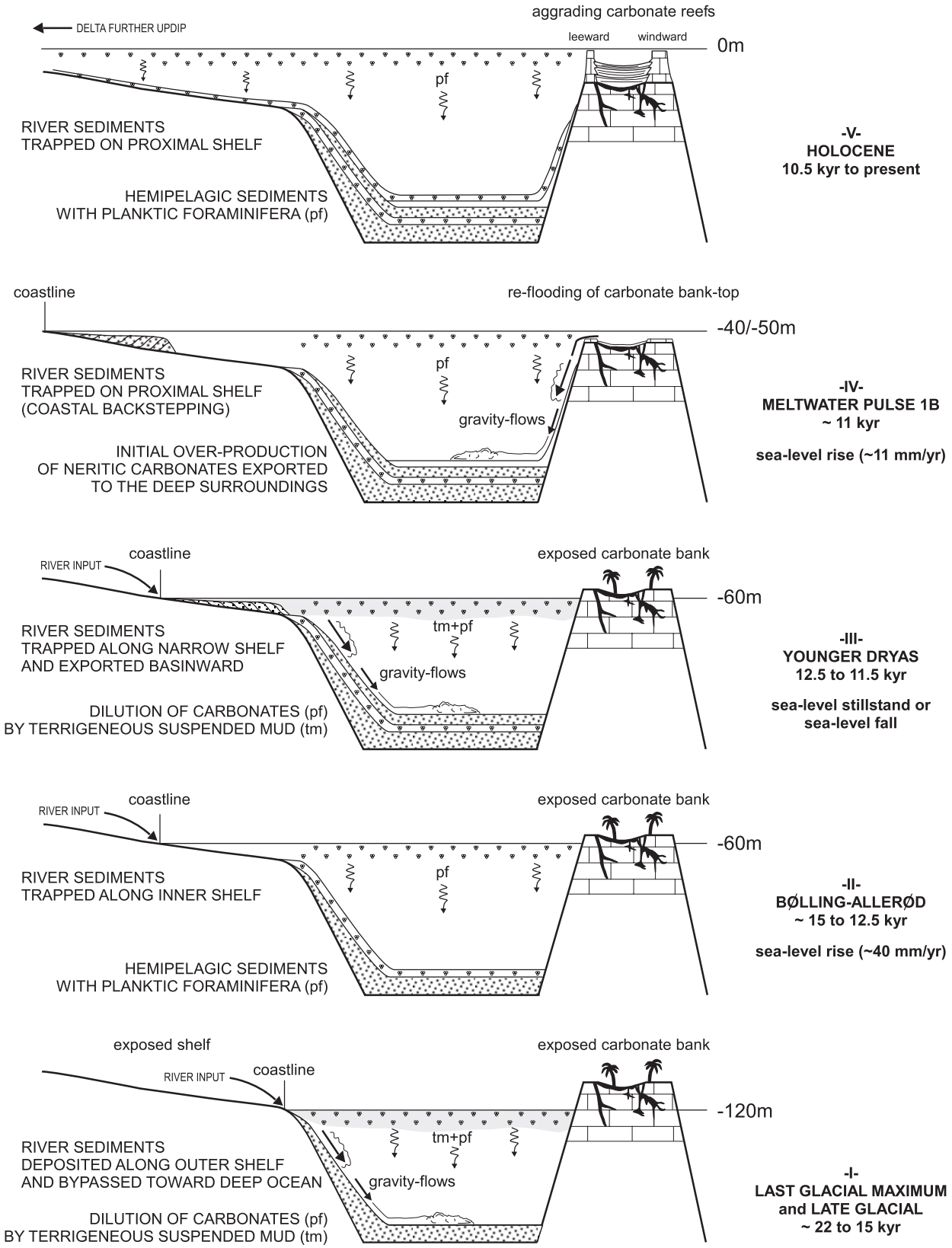
GULF OF PAPUA SHELF
PANDORA TROUGH
EASTERN FIELDS ATOLL
TIME
DELTA FURTHER UPDIP
aggrading carbonate reefs
leeward
windward
0m
pf
RIVER SEDIMENTS TRAPPED ON PROXIMAL SHELF
HEMIPELAGIC SEDIMENTS WITH PLANKTIC FORAMINIFERA (pf)
-V-
HOLOCENE
10.5 kyr to present
coastline
re-flooding of carbonate bank-top
-40/-50m
RIVER SEDIMENTS TRAPPED ON PROXIMAL SHELF (COASTAL BACKSTEPPING)
gravity-flows
INITIAL OVER-PRODUCTION OF NERITIC CARBONATES EXPORTED TO THE DEEP SURROUNDINGS
-IV-
MELTWATER PULSE 1B
~ 11 kyr
sea-level rise (~11 mm/yr)
RIVER INPUT
coastline
exposed carbonate bank
-60m
tm+pf
RIVER SEDIMENTS TRAPPED ALONG NARROW SHELF AND EXPORTED BASINWARD
gravity-flows
DILUTION OF CARBONATES (pf) BY TERRIGENEOUS SUSPENDED MUD (tm)
-III-
YOUNGER DRYAS
12.5 to 11.5 kyr
sea-level stillstand or sea-level fall
RIVER INPUT
coastline
exposed carbonate bank
-60m
pf
RIVER SEDIMENTS TRAPPED ALONG INNER SHELF
HEMIPELAGIC SEDIMENTS WITH PLANKTIC FORAMINIFERA (pf)
-II-
BØLLING-ALLERØD
~ 15 to 12.5 kyr
sea-level rise (~40 mm/yr)
exposed shelf
RIVER INPUT
coastline
exposed carbonate bank
-120m
tm+pf
RIVER SEDIMENTS DEPOSITED ALONG OUTER SHELF AND BYPASSED TOWARD DEEP OCEAN
gravity-flows
DILUTION OF CARBONATES (pf) BY TERRIGENEOUS SUSPENDED MUD (tm)
-I-
LAST GLACIAL MAXIMUM and LATE GLACIAL
~ 22 to 15 kyr

Figure 6

to pelagic sediment with relatively higher carbonate content and the occurrence of a calciturbidite; and (5) interval V, Holocene: devoid of sandy siliciclastic turbidites with rare muddy turbidites, and consists mostly of pelagic sediment rich in carbonate (40–50%) with some bank-derived fine aragonite.

[39] This study in the central part of Pandora Trough includes the first published data set that clearly demonstrates how variations of mixed siliciclastic/carbonate sediment accumulation into a basin adjacent to a siliciclastic shelf and atolls is directly linked to sea level fluctuations during the last deglaciation at millennial timescale variability. Siliciclastic gravity flows occurred during sea level lowstand and stillstand intervals, while they disappear during transgressive and highstand intervals characterized with carbonate enriched hemipelagic sediment. This model is consistent with the basic concept of sequence stratigraphy for siliciclastic sediments, which explains that large quantities of shelf sediments are eroded from the shelf and redeposited on the slopes and in the basins during sea level regression. If rivers reach the shelf edge during maximum lowstand intervals, the entire river load will be accumulated directly on the adjacent slope and basin floor [e.g., *Mitchum*, 1977; *Vail et al.*, 1977; *Vail*, 1987].

[40] The occurrence of the calciturbidite and the onset of bank-derived fine aragonite are contemporaneous to MWP 1B. This observation illustrates that the reflooding of bank tops and margins of adjacent carbonate platforms, such as the modern atolls of Eastern Fields, Portlock, Boot, and Ashmore atolls (with lagoon depths ranging between 40 and 55 m), triggered the reinitiation of neritic carbonate production and export during the transgression following the Younger Dryas (Figure 3). This relationship, well illustrated in central Pandora Trough, is consistent with the concepts of ''highstand shedding'' and ''highstand bundling'' [*Droxler and Schlager*, 1985; *Schlager et al.*, 1994]. These processes explain that carbonate platforms shed sediments produced on their bank tops and edges during the late part of sea level transgressions, as these platform edges and tops are reflooded. Shedding also occurs during highstand intervals, as long as bank tops and/or edges remain within the photic zone after their long-term exposure associated with sea level regressions and lowstands. In the following subsections and Figure 6, a scenario is developed on the basis of the five successive intervals defined in core MD-40 (Figure 3).

5.1. Interval I

[41] During the LGM and late Glacial, the GOP shelf and the bank tops and margins of Eastern Fields, Portlock, Boot, and Ashmore Reefs were subaerially exposed. The lowstand coastal system had migrated all the way to the modern shelf edge [*Droxler et al.*, 2006], and rivers were transporting their sediment loads directly to the upper slope. Isolated carbonate banks were karstified islands. The sediments accumulating into central Pandora Trough were essentially a vertical succession of sandy and muddy siliciclastic turbidites. High volume of the terrigeneous mud released by rivers was transported offshore, diluting the pelagic carbonates.

5.2. Interval II

[42] At the end of the Bølling-Allerød, sea level was ~60 m lower than today. During this 2.0–2.5 ka long interval, sea level had risen by about 50 m, with rates of sea level rise exceeding 40 mm/a. As a direct consequence, the coastline shifted landward and river sediments were trapped on the inner shelf. The Eastern Fields, Ashmore, Boot, and Portlock atolls still remained exposed, and, therefore, continued to be dissolved (karstified). Because of the diminution of the siliciclastic sediments raining through the water column, pelagic sediment enriched in planktic foraminifers and characterized by relatively low accumulation rates represented the main sedimentation in central Pandora. On the slopes, accumulation rates dramatically decreased by a factor 10–20 at the beginning of the Bølling-Allerød [*Febo et al.*, 2008].

5.3. Interval III

[43] The pelagic interval corresponding to the Bølling-Allerød was abruptly interrupted by the return of siliciclastic sandy and muddy turbidites for a short interval that lasted most likely no longer than 1 ka, referred to as the Younger Dryas. During this interval, sea level stopped rising, reaching a stillstand at ~60 m below modern sea level, most likely still too low to flood the bank tops and margins of the modern atolls. However, during the Younger Dryas, influenced by the sea level stillstand (or perhaps an undocumented sea level fall), the siliciclastic coastal system readvanced toward the shelf edge. This movement seaward was enough seaward to bring siliciclastic sandy turbidites into the central Pandora Trough and a large volume of mud close enough to the shelf edge to explain the extreme dilution of the pelagic carbonates at that time.

[44] The Younger Dryas interval was global in nature, because it has been described in the Atlantic basin, on the North and South American continents, in the Sulu Sea [*Kudrass et al.*, 1991; *Linsley and Thunell*, 1990; *de Garidel-Thoron et al.*, 2001], and more recently in the southern Australian Bight [*Andres et al.*, 2003], and in the southwestern tropical Pacific Ocean [*Corrège et al.*, 2004]. Sea-surface temperatures in Vanuatu were on average 4.5 ± 1.3°C cooler during the Younger Dryas interval than today. In Pandora Trough, siliciclastic turbidites were dominant during the late LGM sea level lowstand, and were absent during both meltwater pulses. The occurrence of a major

Figure 6. Two-dimensional diagram illustrating the millennial timescale relationships among variations of sea level, sediment fluxes, and sedimentary processes at the origin of the sedimentary infilling in Pandora Trough from LGM until Holocene. Siliciclastic gravity flows are dominant during LGM, late Glacial, and Younger Dryas and are interrupted by the deposition of hemipelagic carbonate oozes at the Bølling-Allerød warming. The deposition of a calciturbidite in Pandora Trough has been triggered by the reflooding of the Eastern Fields bank top during the MWP 1B, when overproduction of neritic carbonates is exported to the deep ocean. The Eastern Fields Holocene atoll is characterized by an aggrading rimmed carbonate platform, where exceeding sediment is preferentially trapped in the lagoon.

siliciclastic turbidite at the beginning of the Younger Dryas can be explained by cooling with no change in sea level. It implies that a humid climate can trigger erosion on the land, accumulation of terrigeneous sediment on a reduced shelf area (sea level was 60 m lower than today), and export of siliciclastic gravity flows toward the slope and the basin. Although no direct lines of evidence for a Younger Dryas sea level fall have been observed in spite of the significant advance of the Fennoscandian ice sheet during that particular interval [*Mangerud et al.*, 1979], R. G. Fairbanks (personal communication, 2006) does not rule out such a sea level fall, in particular, because a drop of sea level is now observed during the Oldest Dryas [*Peltier and Fairbanks*, 2006]. On the basis of sedimentological arguments, our study from Pandora trough would support this suggested sea level fall during the Younger Dryas.

5.4. Interval IV

[45] Siliciclastic sandy and muddy turbidites were shut down by the rapid 15–20 m sea level rise (11 mm/a) during MWP 1B, and never returned to the central part of Pandora Trough during the Holocene. Their absence eliminated siliciclastic sands and the majority of the mud from the outer shelf and, therefore, the central part of Pandora Trough. The sediment in the trough became relatively enriched in carbonates as sea level flooded the margins and tops of the modern atolls, supplying bank-derived aragonite in the fine sediment fraction, dated at ~12 ka B.P.

5.5. Interval V

[46] The rest of the Holocene is characterized by an increase of the carbonate content (coccoliths and planktic foraminifers) in the pelagic sediment. The typical atoll modern morphology is reinforced by their rim aggradation during the Holocene transgression, causing loose neritic sediments to accumulate either in the lagoon or on the slope and basin floors adjacent to the atolls.

6. Conclusions

[47] The study of three cores collected in the central part of Pandora Trough reveals a detailed sedimentary pattern at millennial timescale during the last glacial/interglacial cycle. This sedimentary variability at millennium scale demonstrates that the last glacial-interglacial transition was a two-step change from the Last Glacial Maximum to the Holocene. The deposition of a pelagic carbonate interval during the Bølling-Allerød, devoid of sandy and muddy turbidites, marked the first step of deglaciation. The second step corresponded to the deposition of a calciturbidite during the meltwater pulse 1B. This two-step deglaciation was clearly interrupted by the deposition of siliciclastic sandy and muddy turbidites during the Younger Dryas cold reversal.

[48] The observed millennial timescale sedimentary variability can be explained by the sea level fluctuations corresponding to maximum rates of sea level rise (meltwater pulses 1A and 1B, <40 mm/a, and 11 mm/a, respectively) and to a one 1 ka cooling interval of the Younger Dryas. The input of siliciclastic turbidites was maximal during Last Glacial Maximum, when the lowstand coastal system was located along the modern continental shelf edge, and disappeared during the intervals of maximum reflooding of the shelf during meltwater pulses 1A and 1B. Siliciclastic turbidites reappeared briefly during the Younger Dryas, an interval when rates of sea level rise slowed down or most likely stopped. The timing of the calciturbidite coincided with the first reflooding of Ashmore, Boot, Portlock, and Eastern Fields atoll during the meltwater pulse 1B. It represents the initiation of neritic carbonate production of the bank top, which had remained exposed for most of the glacial stages. The deposition of this calciturbidite (~11 ka B.P.) strongly suggests that carbonate production started very rapidly during the second step of the deglaciation.

[49] **Acknowledgments.** This research was supported by the National Science Foundation (OCE 0305688), the Swiss National Foundation (PBGE2-111250), and by TOTAL (R62620). We are grateful to the captains, officers, crew members, and scientific and technical shipboard parties of the PANASH cruise on the R/V *Melville* part of NSF MARGINS Source-to-Sink initiative and the PECTEN cruise on the R/V *Marion Dufresne* part of an IMAGES cruise. IPEV (Institut Polaire Paul-Emile Victor) and in particular Yvon Balut are acknowledged for support in recovering high-quality cores with R/V *Marion Dufresne*. We are grateful to David Winter (UC Davis) who ran oxygen isotopes analyses and Guaciara Dos Santos (University of California) for radiocarbon AMS dates. We acknowledge Philippe Lapointe at TOTAL for his continuous support and interest and for the funding of the TOC analyses. We thank Chuck Nittrouer, Bill Normack, and Chris Goldfinger for constructive comments on an earlier draft of this paper.

References

Alley, R. B., et al. (1993), Abrupt increase in Greenland snow accumulation at the end of the Younger Dryas event, *Nature*, *362*, 527–529.

Anderson, D. M., W. L. Prell, and N. J. Barratt (1989), Estimates of sea surface temperature in the Coral Sea at the Last Glacial Maximum, *Paleoceanography*, *4*, 615–627.

Andres, M. S., S. M. Bernasconi, J. A. Mc Kenzie, and U. Rohl (2003), Southern Ocean deglacial record supports global Younger Dryas, *Earth Planet. Sci. Lett.*, *216*, 515–524.

Andresen, N., J. J. G. Reijmer, and A. W. Droxler (2003), Timing and distribution of calciturbidites around a deeply submerged carbonate platform in a seismically active setting (Pedro Bank, Northern Nicaragua Rise Caribbean Sea), *Int. J. Earth Sci.*, *92*, 573–592.

Bard, E., B. Hamelin, R. G. Fairbanks, and A. Zindler (1990), Calibration of the ^{14}C timescale over the past 30,000 years using mass spectrometric U–Th ages from Barbados corals, *Nature*, *345*, 405–410.

Bard, E., M. Arnold, J. Mangerud, M. Paterne, L. D. Labeyrie, J. Duprat, E. Melieres, E. Sønstegaard, and J. C. Duplessy (1994), The North Atlantic atmosphere-sea surface ^{14}C gradient during the Younger Dryas climatic event, *Earth Planet. Sci. Lett.*, *126*, 257–287.

Bassett, S. E., G. A. Milne, J. X. Mitrovica, and P. U. Clark (2005), Ice sheet and solid earth influences on far-field sea-level histories, *Science*, *309*, 925–928.

Belopolsky, A. V., and A. W. Droxler (1999), Uppermost Pleistocene transgressive coralgal reefs on the edge of the South Texas Shelf: Analogs for reefal reservoirs buried in siliciclastic shelves, paper presented at 19th Annual Research Conference Advanced Reservoir Characterization, Golf Coast Sect. of the Soc. of Econ. Paleontol. and Mineral. Found., Houston, Tex.

Bouma, A. H. (1982), Intraslope basins in northwest Gulf of Mexico: A key to ancient submarine canyons and fans, in *Studies in Continental Margin Geology*, *Am. Assoc. of Pet. Geol. Mem. Ser.*, vol. 34, edited by J. S. Watkins and C. L. Drake, pp. 567–581, Am. Assoc. of Pet. Geol., Tulsa, Okla.

Budd, D. A., and P. M. Harris (Eds.) (1990), *Carbonate-Siliciclastic Mixtures*, *SEMP Reprint Ser.*, vol. 14, 272 pp., Soc. of Sediment. Geol., Tulsa, Okla.

Carson, B., J. Francis, R. Leckie, A. Doxler, G. R. Dickens, S. J. Jorry, S. J. Bentley, L. C. Peterson, and B. Opdyke (2008), Benthic foraminiferal response to sea level change in the mixed siliciclastic-carbonate system of the southern Ashmore Trough (Gulf of Papua), *J. Geophys. Res.*, doi:10.1029/2006JF000629, in press.

Chodankar, A. R., V. K. Banakar, and T. Oba (2005), Past 100 ky surface salinity-gradient response in the eastern Arabian Sea to the summer monsoon variation recorded by delta (super 18) O of *G. sacculifer*, *Global Planet. Change*, *47*, 135–142.

Clark, P. U., A. Marshall, A. McCabe, A. C. Mix, and A. J. Weaver (2004), Rapid rise of sea level 19000 years ago and its global implications, *Science*, *304*, 1141–1144.

Corrège, T., M. K. Gagan, J. W. Beck, J. S. Burr, G. Cabioch, and F. Le Cornec (2004), Interdecadal variation in the extent of South Pacific tropical waters during the Younger Dryas event, *Nature*, *428*, 927–929.

de Garidel-Thoron, T., L. Beaufort, B. K. Linsley, and S. Dannenmann (2001), Millennial-scale dynamics of the east Asian winter monsoon during the last 200,000 years, *Paleoceanography*, *16*, 1–12.

de Garidel-Thoron, T., L. Beaufort, F. Bassinot, and P. Henry (2004), Evidence for large methane releases to the atmosphere from deep-sea gas-hydrate dissociation during the last glacial episode, *Proc. Natl. Acad. Sci. U. S. A.*, *101*, 9187–9192.

Droxler, A. W., and W. Schlager (1985), Glacial versus interglacial sedimentation rates and turbidite frequency in the Bahamas, *Geology*, *13*, 799–802.

Droxler, A. W., J. W. Morse, and W. A. Kornicker (1988), Controls on carbonate mineral accumulation in Bahamian basins and adjacent Atlantic Ocean sediments, *J. Sediment. Res.*, *58*, 120–130.

Droxler, A. W., G. Mallarino, J. M. Francis, G. J. Dickens, B. N. Opdyke, L. Beaufort, J. Daniell, S. J. Bentley, and L. C. Peterson (2006), Early transgressive establishment of relict uppermost Pleistocene barrier reefs on LGM coastal siliciclastic deposits in the Gulfs of Papua and Mexico: Clue to understand the Mid-Brunhes origin of modern barrier reefs, in *AAPG Meeting: Abstract Book*, vol. 55, pp. 37–38, Am. Assoc. of Pet. Geol., Tulsa, Okla.

Dürkoop, A., W. Hale, S. Mulitza, J. Pätzold, and G. Wefer (1997), Late Quaternary variations of sea surface salinity and temperature in the western tropical Atlantic: Evidence from ä^{18}O of *Globigerinoides Sacculifer*, *Paleoceanography*, *12*, 764–772.

Dunbar, G. B., G. R. Dickens, and R. M. Carter (2000), Sediment flux across the Great Barrier Reef Shelf to the Queensland Trough over the last 300 ky, *Sediment. Geol.*, *133*, 49–92.

Duplessy, J.-C., E. Bard, M. Arnold, N. J. Shackleton, J. Duprat, and L. Labeyrie (1991), How fast did the ocean-atmosphere system run during the last deglaciation?, *Earth Planet. Sci. Lett.*, *103*, 27–40.

Edwards, R. L., J. W. Beck, G. S. Burr, D. J. Donahue, J. M. A. Chappell, A. L. Bloom, E. R. M. Druffel, and F. W. Taylor (1993), A large drop in atmospheric $^{14}C/^{12}C$ and reduced melting in the Younger Dryas, documented with ^{230}Th ages of corals, *Science*, *260*, 962–968.

Fairbanks, R. G. (1989), A 17,000 year glacio-eustatic sea level record; influence of glacial melting rates on the Younger Dryas event and deep ocean circulation, *Nature*, *342*, 637–642.

Fairbanks, R. G., R. A. Mortlock, T. C. Chiu, L. Cao, A. Kaplan, T. P. Guilderson, T. W. Fairbanks, A. L. Bloom, P. M. Grootes, and M. J. Nadeau (2005), Radiocarbon calibration curve spanning 0 to 50000 years BP based on paired $^{230}Th/^{234}U/^{238}U$ and ^{14}C dates on pristine corals, *Quat. Sci. Rev.*, *24*, 1781–1796.

Febo, L. A., S. J. Bentley, J. H. Wrenn, A. W. Droxler, G. R. Dickens, L. C. Peterson, and B. Opdyke (2008), Late Pleistocene and Holocene sedimentation, organic-carbon delivery, and paleoclimatic inferences on the continental slope of the northern Pandora Trough, Gulf of Papua, *J. Geophys. Res.*, doi:10.1029/2006JF000677, in press.

Ferro, C. E., A. W. Droxler, J. B. Anderson, and D. Mucciarone (1999), Late Quaternary shift of mixed siliciclastic-carbonate environments induced by glacial eustatic sea-level fluctuations in Belize, in *Advances in Carbonate Sequence Stratigraphy: Application to Reservoirs, Outcrops, and Models*, *SEMP Spec. Publ.*, vol. 63, edited by P. M. Harris, A. H. Saller, and J. A. Simo, pp. 385–411, Soc. of Sediment. Geol., Tulsa, Okla.

Foreman, J. L., K. R. Walker, L. J. Weber, S. G. Driese, and R.B. Dreier (1991), Slope and basinal carbonate deposition in the Nolichucky Shale (Upper Cambrian), east Tennessee: Effect of carbonate suppression by siliciclastic deposition on basin-margin morphology, in *Mixed Carbonate-Siliciclastic Sequences*, *SEMP Core Workshop Ser.*, vol. 15, edited by A. J. Lomando and P. M. Harris, pp. 511–539, Tulsa, Okla.

Francis, J., J. J. Daniell, A. W. Droxler, G. R. Dickens, S. J. Bentley, L. C. Peterson, B. Opdyke, and L. Beaufort (2008), Deepwater geomorphology of the mixed siliciclastic-carbonate system, Gulf of Papua, *J. Geophys. Res.*, doi:10.1029/2007JF000851, in press.

Gibbs, R. J. (1981), Sites of river-derived sedimentation in the ocean, *Geology*, *9*, 77–80.

Gischler, E. (2003), Holocene lagoonal development in the isolated carbonate platforms off Belize, *Sediment. Geol.*, *159*, 113–132.

Glaser, K. S., and A. W. Droxler (1993), Controls and development of late Quaternary periplatform carbonate stratigraphy in Walton Basin (Northern Nicaragua Rise Caribbean Sea), *Paleoceanography*, *8*, 243–274.

Goldsmith, J. R., D. L. Graf, and H. C. Heard (1961), Lattice constants of the calcium magnesium carbonates, *Am. Mineral.*, *46*, 453–457.

Grootes, P. M., M. Stuiver, J. W. C. White, S. Johnsen, and J. Jouzel (1993), Comparison of oxygen isotope records from the GISP2 and GRIP Greenland ice cores, *Nature*, *366*, 552–554.

Guilderson, T., R. G. Fairbanks, and J. Rubenstone (2001), Tropical Atlantic coral oxygen isotopes; glacial-interglacial sea surface temperatures and climate change, *Mar. Geol.*, *172*, 75–89.

Hanebuth, T., K. Stattegger, and P. M. Grootes (2000), Rapid flooding of the Sunda Shelf: A late glacial sea-level record, *Science*, *288*, 1033–1035.

Harris, P. T., E. K. Baker, A. R. Cole, and S. A. Short (1993), A preliminary study of sedimentation in the tidally dominated Fly River delta, *Gulf of Papua, Cont. Shelf Res.*, *13*, 441–472.

Harris, P. T., C. B. Pattiaratchi, J. B. Keene, R. W. Dalrymple, J. V. Gardner, E. K. Baker, A. R. Cole, D. Mitchell, P. Gibbs, and W. W. Schroeder (1996), Late Quaternary deltaic and carbonate sedimentation in the Gulf of Papua foreland basin: Response to sea-level change, *J. Sediment. Res.*, *66*, 801–819.

Holmes, A. E., and N. Christie-Blick (1993), Origin of sedimentary cycles in mixed carbonate-siliciclastic systems: An example from the Canning Basin, Western Autralia, in *Carbonate Sequence Stratigraphy: Recent Developments and Applications*, *Am. Assoc. of Pet. Geol. Mem. Ser.*, vol. 57, edited by R. G. Loucks and J. F. Sarg, pp. 181–212, Tulsa, Okla.

Hughen, K. A., J. R. Southon, S. J. Lehman, and J. T. Overpeck (2000), Synchronous radiocarbon and climate shifts during the last deglaciation, *Science*, *190*, 1951–1954.

Kienast, M., T. J. J. Hanebuth, C. Pelejero, and S. Steinke (2003), Synchroneity of meltwater pulse 1a and the Bølling warming: New evidence from the South China Sea, *Geology*, *31*, 67–70.

Kudrass, H. R., H. Erlenkeuser, R. Vollbrecht, and W. Weiss (1991), Global nature of the Younger Dryas cooling event inferred from oxygen isotope data from Sulu sea cores, *Nature*, *349*, 406–409.

Lambeck, K., and J. Chappell (2001), Sea level change through the last glacial cycle, *Science*, *292*, 679–686.

Lambeck, K., T. M. Esat, and E. K. Potter (2002), Links between climate and sea levels for the past three million years, *Nature*, *419*, 199–206.

Lea, D. W., D. K. Pak, and H. J. Spero (2000), Climate impact of late Quaternary equatorial Pacific sea surface temperature variations, *Science*, *289*, 1719–1724.

Lea, D. W., P. A. Martin, D. K. Pak, and H. J. Spero (2002), Reconstructing a 350 ky history of sea level using planktic Mg/Ca and oxygen isotope records from a Cocos Ridge core, *Quat. Sci. Rev.*, *21*, 283–293.

Linsley, B. K. (1996), Oxygen-isotope record of climate and sea-level variations in the Sulu Sea over the past 150000 years, *Nature*, *380*, 234–237.

Linsley, B. K., and R. C. Thunell (1990), The record of deglaciation in the Sulu Sea: Evidence for the Younger Dryas event in the tropical western Pacific, *Paleoceanography*, *5*, 1025–1039.

Liu, J. P., J. D. Milliman, S. Gao, and P. Cheng (2004), Holocene development of the Yellow River's subaqueous delta, North Yellow Sea, *Mar. Geol.*, *209*, 45–67.

MacKinnon, L., and B. Jones (2001), Sedimentological evolution of North Sound, Grand Cayman: A freshwater to marine carbonate succession driven by Holocene sea-level rise, *J. Sediment. Res.*, *71*, 568–580.

Mallarino, G., R. T. Beaubouef, A. W. Droxler, V. Abreu, and L. Labeyrie (2006), Sea-level influence on the nature and timing of a minibasin sedimentary fill (northwestern slope of the Gulf of Mexico), *AAPG Bull.*, *90*, 1089–1119.

Mangerud, J., E. Larsen, O. Longva, and E. Sønstegaard (1979), Glacial history of western Norway 15000–10000 BP, *Boreas*, *8*, 179–187.

Mitchum, R. M. (1977), Seismic stratigraphy and global changes of sea level: Part 11, Glossary of terms used in seismic stratigraphy, in *Seismic Stratigraphy: Applications to Hydrocarbon Exploration*, *Am. Assoc. of Pet. Geol. Mem. Ser.*, vol. 26, edited by C. E. Payton, pp. 205–212, Am. Assoc. of Pet. Geol., Tulsa, Okla.

Mount, J. F. (1984), Mixing of siliciclastic and carbonate sediments in shallow shelf environments, *Geology*, *12*, 432–435.

Müller, G., and M. Gastner (1971), The ''karbonat-bombe'': A simple device for the determination of the carbonate content in sediments, soils, and other materials, *Neues Jahrb. Mineral. Abh.*, *10*, 466–469.

Page, M. C., G. R. Dickens, and G. B. Dunbar (2003), Tropical view of Quaternary sequence stratigraphy: Siliciclastic accumulation on slopes east of the Great Barrier Reef since the Last Glacial Maximum, *Geology*, *31*, 1013–1016.

Peltier, W. R., and R. G. Fairbanks (2006), Global glacial ice volume and Last Glacial Maximum duration from an extended Barbados sea level record, *Quat. Sci. Rev.*, *25*, 3322–3337, doi:10.1016/j.quascirev.2006.04.010.

Pickup, G., and V. H. Chewings (1983), The hydrology of the Purari and its environmental implications, in *The Purari: Tropical Environment of a*

High Rainfall River Basin, edited by T. Petr, pp. 123–140, Springer, New York.

Reimer, P. J., and R. W. Reimer (2001), A marine reservoir correction database and on-line interface, *Radiocarbon*, *43*, 461–463. (Supplemental material available at http://www.calib.org.)

Salomons, W. A. M., and A. M. Eagle (1990), Hydrology, sedimentology, and the fate and distribution of copper in mine-related discharges in the Fly River system, Papua New Guinea, *Sci. Total Environ.*, *97/98*, 345–513.

Schlager, W., J. J. G. Reijmer, and A. W. Droxler (1994), Highstand shedding of carbonate platforms, *J. Sediment. Res.*, *64*, 270–281.

Stott, L., C. Poulsen, S. Lund, and R. Thunell (2002), Super ENSO and global climate oscillations at millennial time scales, *Science*, *297*, 222–226.

Stuiver, M., and T. F. Braziunas (1993), Modeling atmospheric ^{14}C influences and ^{14}C ages of marine samples to 10000 BC, *Radiocarbon*, *35*, 137–189.

Stuiver, M., and P. M. Grootes (2000), GISP2 Oxygen Isotope Ratios, *Quat. Res.*, *53*, 277–284.

Tcherepanov, E., A. W. Droxler, P. Lappointe, G. R. Dickens, S. J. Bentley, L. Beaufort, L. C. Peterson, J. J. Daniell, and B. Opdyke (2008), Neogene evolution of the mixed carbonate-siliciclastic system in the Gulf of Papua, Papua New Guinea, *J. Geophys. Res.*, *113*, F01S21, doi:10.1029/2006JF000684.

Thunell, R. C., D. M. Anderson, D. Gellar, and Q. Miao (1994), Sea-surface temperature estimates for the tropical western Pacific during the last glaciation and their implications for the Pacific warm pool, *Quat. Res.*, *41*, 255–264.

Vail, P. R. (1987), Seismic stratigraphy interpretation procedure, in *Atlas of Seismic Stratigraphy*, *Am. Assoc. of Pet. Geol. Stud. Geol. Ser.*, vol. 27, edited by A. W. Bally, pp. 1–10, Am. Assoc. of Pet. Geol., Tulsa, Okla.

Vail, P. R., R. M. Mitchum, and S. Thompson (1977), Global cycles of relative changes of sea level, in *Seismic Stratigraphy: Applications to Hydrocarbon Exploration*, *Am. Assoc. of Pet. Geol. Mem. Ser.*, vol. 26, edited by C. E. Payton, pp. 83–97, Am. Assoc. of Pet. Geol., Tulsa, Okla.

Visser, K., R. C. Thunell, and L. Stott (2003), Magnitude and timing of temperature change in the Indo-Pacific warm pool during deglaciation, *Nature*, *421*, 152–155.

Walsh, J. P., and C. A. Nittrouer (2004), Mangrove-bank sedimentation in a mesotidal environment with large sediment supply, *Gulf of Papua, Mar. Geol.*, *208*, 225–248.

Weaver, A. J., O. A. Saenko, P. U. Clark, and J. X. Mitrovica (2003), Meltwater pulse 1A from Antarctica as a trigger of the Bølling-Allerød warm interval, *Science*, *299*, 1709–1713.

Yokoyama, Y., K. Lambeck, P. De Deckker, P. Johnston, and K. Fifield (2000), Timing of the Last Glacial Maximum from observed sea-level minima, *Nature*, *406*, 713–716.

L. Beaufort, Clouds and the Earth's Radiant Energy System, CNRS, Université Aix-Marseille III, BP80, F-13545 Aix-en-Provence cedex 4, France. (beaufort@cerege.fr)

S. J. Bentley, Earth Sciences Department, Memorial University of Newfoundland, St John's, NL, Canada A1B 3X5. (sjb@esd.mun.ca)

G. R. Dickens and A. W. Droxler, Department of Earth Science, Rice University, 6100 Main Street, Houston, TX 77005-1892, USA. (andre@rice.edu; jerry@rice.edu)

S. J. Jorry, Beicip-Franlab Petroleum Consultants, 232 Avenue Napoléon Bonaparte, F-92500 Rueil-Malmaison, France. (stephan.jorry@beicip.com)

G. Mallarino, PanTerra Geoconsultants B.V., Weversbaan 1-3, NL-2352 BZ Leiderdorp, Netherlands. (g.mallarino@panterra.nl)

B. N. Opdyke, Department of Earth and Marine Sciences, Australian National University, Canberra, ACT 0200, Australia. (bradley.opdyke@anu.edu)

L. C. Peterson, Rosentiel School of Marine and Atmospheric Science, University of Miami, Miami, FL 33149, USA. (lpeterson@rsmas.miami.edu)